

Grafting polymers onto carbon black surface by trapping polymer radicals

Qiang Yang^a, Li Wang^{a,*}, Weidong Xiang^b, Junfeng Zhou^a, Jianhua Li^a

^a *The State Key Laboratory of Polymer Reaction Engineering, College of Materials Science and Chemical Engineering, Zhejiang University, Hangzhou 310027, People's Republic of China*

^b *College of Applied Technology, Wenzhou University, Wenzhou 325035, People's Republic of China*

Received 11 September 2006; received in revised form 21 December 2006; accepted 23 January 2007

Available online 14 February 2007

Abstract

Polystyrene, poly(styrene-*co*-maleic anhydride), poly[styrene-*co*-(4-vinylpyridine)] and poly(4-vinylpyridine) with well-defined molecular weights and polydispersities were synthesized using 4-hydroxyl-2,2,6,6-tetramethylpiperidin-1-oxyl (HTEMPO)-mediated radical polymerization initiated by azobisisobutyronitrile or benzoyl peroxide. The resultant polymers were grafted onto carbon black surface through a radical trapping reaction at 130 °C in DMF. ¹H NMR, TGA, TEM, AFM, DSC and dynamic light scattering were used to characterize the carbon black grafted with polymers. It was found that the carbon black grafted with polystyrene and poly(styrene-*co*-maleic anhydride) could be dispersed in THF, chloroform, dichloromethane, DMF, etc., and the carbon black grafted with poly(4-vinylpyridine) and poly[styrene-*co*-(4-vinylpyridine)] could be well dispersed in ethanol.

© 2007 Published by Elsevier Ltd.

Keywords: HTEMPO; Radical trapping; Carbon black

1. Introduction

Carbon black/polymer composites are used as gas sensing materials to detect, quantify and discriminate various organic vapors [1–6]. In the carbon black/polymer composites, selective adsorption of polymer on the carbon black surface often leads to a heterogeneous dispersion of carbon black particles in the polymer matrix as a result of a very low percolation threshold [7]. Carbon black grafted with polymer may be one of more practicable gas sensor materials because of the improved dispersion in polymer matrix or solvent leading to better response behaviors. There are two kinds of polymer grafting methods including “grafting from” and “grafting to”. The “grafting from” approach means grafting polymers from carbon black surface. The “grafting from” approach can bring about a higher grafting polymer density, nevertheless initiator

groups such as $-\text{CH}_2\text{OH}$, $-\text{OLi}$, $-\text{COO}^- \text{M}^+$, $-\text{CO}^+ \text{ClO}_4^-$, $-\text{NH}_2$, peroxyesters or azo moieties should be introduced onto carbon black surface before grafting polymerization. In the past decades, most research focused on anionic polymerization [8], cationic polymerization [9–11], surface-initiated ring-opening polymerization (SI-ROP) [12–14], and radical polymerization on the carbon black surface [15]. In recent years, surface-initiated atom transfer radical polymerization (SI-ATRP) has proved to be a promising living/controlled free radical polymerization and has been used to modify and functionalize nanoparticles. Jin et al. grafted polymers onto carbon spheres by SI-ATRP [16]. Li and Lukehart synthesized hydrophobic and hydrophilic graphitic carbon nanofiber with polymer brushes by SI-ATRP [17]. Matyjaszewski and co-workers reported that after the C–Br bond attached onto carbon black surface, the SI-ATRP of *n*-butyl acrylate, *t*-butyl acrylate and 2-(dimethylamino) ethyl methacrylate could be successfully carried out [18–20]. However, the “grafting to” method is to graft polymer through a reaction between

* Corresponding author. Tel.: +86 571 87953200; fax: +86 571 87951612.
E-mail address: opl_wl@diel.zju.edu.cn (L. Wang).

carbon black and end-functionalized polymer or trapping polymer radicals [21–23]. Although a relatively low grafting polymer density is obtained due to the steric hindrance from the previous grafted polymer chains, the “grafting to” method is simple and practical one. Nitroxide-mediated radical polymerization has proved to be a feasible method to prepare 2,2,6,6-tetramethylpiperidin-1-oxyl (TEMPO)-terminated polymers with controlled molecular weights and polydispersities. Adronov and coworkers functionalized single-walled carbon nanotubes with well-defined polymers by radical coupling [24]. Tsubokawa and coworkers reported grafting polystyrene with controlled molecular weight and polydispersity onto carbon black surface through trapping of the polymer radicals formed by thermal dissociation of TEMPO-terminated polystyrene [21]. Chiu et al. also synthesized five kinds of TEMPO-terminated polymers and grafted them onto carbon black surface by radical trapping method [22].

Polymers with controlled molecular weights and polydispersities can be also synthesized using 4-hydroxyl-2,2,6,6-tetramethylpiperidin-1-oxyl (HTEMPO)-mediated radical polymerization [25–28]. In this paper, four kinds of HTEMPO-terminated polymers involving polystyrene, poly(4-vinylpyridine), poly(styrene-co-maleic anhydride) and poly[styrene-co-(4-vinylpyridine)] were prepared using HTEMPO-mediated radical polymerization initiated by azobisisobutyronitrile or benzoyl peroxide. The resultant HTEMPO-terminated polymers were grafted onto carbon black surface through radical trapping method. Carbon black grafted with these polymers is characterized here systematically and the mechanism of trapping polymers by carbon black surface is also discussed in detail.

2. Experimental part

2.1. Materials

Primary carbon black particles (CB, VXC 605), with an average size of 30 nm and a specific surface area of 254 m²/g, were obtained from Cabot. 4-Vinylpyridine (4VP) and styrene (St) were distilled before use. Azobisisobutyronitrile (AIBN) and benzoyl peroxide (BPO) were purified by recrystallization in anhydrous methanol. Maleic anhydride (MA) was used as received. 4-Hydroxyl-2,2,6,6-tetramethylpiperidin-1-oxyl (HTEMPO) was bought from Acros and purified by recrystallization in hexane.

2.2. Synthesis of HTEMPO-PS [25]

Styrene (10 ml, 87.4 mmol), AIBN (98.5 mg, 0.6 mmol) and HTEMPO (103.8 mg, 0.6 mmol) were added into a two-necked flask, degassed with three freeze–thaw cycles. Under magnetic stirring, the reaction mixture was first preheated to 95 °C for 1 h to allow for the decomposition of AIBN and then was heated up to 125 °C. After reaction for 7 h, the product was precipitated in ethanol and was dried in vacuum at 50 °C. Yield: 75%; $M_n = 7.42 \times 10^3$, PDI = 1.15.

¹H NMR (CDCl₃) δ (ppm): 7.20–6.30 (–C₆H₅), 2.25–1.74 (–CH (C₆H₅)), 1.74–1.25 (–CH₂–CH (C₆H₅)).

2.3. Synthesis of HTEMPO-P(St-co-MA) [26]

Styrene (5 ml, 43.7 mmol), MA (0.4285 g, 4.37 mmol), HTEMPO (51.2 mg, 0.297 mmol) and BPO (40 mg, 165 μ mol) were added into a two-necked flask, degassed with three freeze–thaw cycles. Under magnetic stirring, the reaction mixture was first preheated to 100 °C for 1 h to allow the decomposition of BPO and then was heated up to 125 °C. After reaction for 7 h, the product was precipitated in methanol and was dried in vacuum at 50 °C. Yield: 78%; $M_n = 3.5 \times 10^3$, PDI = 1.41.

¹H NMR (CDCl₃) δ (ppm): 7.22–6.29 (–C₆H₅), 2.22–1.67 (–CH (C₆H₅)), 1.67–1.14 (–CH₂–CH (C₆H₅)).

2.4. Synthesis of HTEMPO-P(St-co-4VP) [27]

Styrene (5.72 ml, 50 mmol), 4-vinylpyridine (2.28 ml, 21.7 mmol), HTEMPO (67.4 mg, 0.36 mmol) and AIBN (28.5 mg, 0.2 mmol) were added into a two-necked flask, degassed with three freeze–thaw cycles. Under magnetic stirring, the reaction mixture was first preheated to 100 °C for 2 h to allow for the decomposition of AIBN and then was heated up to 125 °C. After reaction for 36 h, the product was precipitated in ether and was dried in vacuum at 50 °C. Yield: 82%; $M_n = 8.1 \times 10^3$, PDI = 1.27.

¹H NMR (CDCl₃) δ (ppm): 8.48–8.02 (–CH–N–CH–), 7.23–6.09 (–CH–C–CH–), 2.31–1.57 (–CH₂–CH–), 1.57–1.06 (–CH₂–CH–).

2.5. Synthesis of HTEMPO-P4VP [28]

4-Vinylpyridine (3 ml, 28.5 mmol), BPO (13.4 mg, 55.3 μ mol) and HTEMPO (12.4 mg, 72.1 μ mol) were added into a two-necked flask, degassed with three freeze–thaw cycles. Under magnetic stirring, the reaction mixture was first preheated to 100 °C for 1 h to allow for the decomposition of BPO and then was heated up to 125 °C. After reaction for 26 h, the product was precipitated in ether and was dried in vacuum at 50 °C. Yield: 79%; $M_n = 8.3 \times 10^3$, PDI = 1.20.

¹H NMR (CDCl₃) δ (ppm): 8.76–7.97 (–CH–N–CH–), 7.23–6.09 (–CH–C–CH–), 2.24–1.75 (–CH₂–CH–), 1.75–1.18 (–CH₂–CH–).

2.6. Synthesis of CB-g-polymer

Taking CB-g-PS (CB-g-PS-3 in Table 1) as an example, a typical reaction is done as follows. CB (50.4 mg), DMF (5 ml) and HTEMPO-PS (0.2045 g, 27.6 μ mol) were added into a two-necked flask, degassed with three freeze–thaw cycles. Under magnetic stirring, the reaction mixture was heated at 130 °C for 12 h. At the end of the reaction, the grafted carbon black was separated centrifugally and was washed with THF for three times (each time was 30 min, rotation speed was 3000 rpm) to remove any possible absorbed un-grafted

Table 1
Reaction conditions and results

Sample	Time (h)	Polymer (%)	Particle size (nm)
CB-g-PS-1	3	4.44	138
CB-g-PS-2	6	9.79	179
CB-g-PS-3	12	14.04	185
CB-g-PS-4	24	19.60	193
CB-g-P(St-co-MA)-1	3	4.88	126
CB-g-P(St-co-MA)-2	6	7.16	155
CB-g-P(St-co-MA)-3	12	13.35	176
CB-g-P(St-co-MA)-4	24	31.76	198

Reaction conditions: temperature = 130 °C, the weight ratio of HTEMPO-polymer/carbon black (w/w) = 4, CB = 50 mg, DMF = 5 ml. HTEMPO-PS: $M_n = 7.42 \times 10^3$, PDI = 1.15, determined by GPC; HTEMPO-P(St-co-MA): $M_n = 3.5 \times 10^3$, PDI = 1.41, determined by GPC. Polymer (%) = the polymer content, calculated from TGA under N_2 . Particle size was measured from dynamic light scattering in THF.

polystyrene. The resultant product was dried in vacuum at 50 °C. Yield: 80%.

1H NMR ($CDCl_3$) δ (ppm): 7.20–6.30 ($-C_6H_5$), 2.25–1.74 ($-CH$ (C_6H_5)), 1.74–1.25 ($-CH_2-CH$ (C_6H_5)).

2.7. Characterizations

1H NMR spectra were recorded with a 400 MHz AVANCE NMR spectrometer (Model DMX400) in $CDCl_3$ using TMS as the standard. Thermogravimetric (TGA) curves were obtained from a Perkin–Elmer Pyris thermogravimetric instrument, at a heating rate of 20 °C/min from 25 °C to 800 °C in a flow of nitrogen. Glass transition temperature (T_g) was recorded on a Perkin–Elmer DSC-7 differential scanning calorimeter (DSC) at a heating rate of 20 °C/min. Molecular weights of HTEMPO-terminated polymers were determined by gel permeation chromatography (GPC) with laser scattering detector, ultrastayragel column with pore sizes of 10^3 – 10^5 Å. Dynamic light scattering (DLS) experiments were performed on a Zetasizer 3000 HSA (Malvern Instruments, Ar-laser, wavelength 633 nm, count rate 240.9, cell type capillary cell, power 70 mW, detector angle 90 °, 25 °C). Transmission electron microscopy (TEM) images were obtained from a JEOL model 1200EX instrument operated at an accelerating voltage of

160 kV. Atomic force microscopy (AFM) measurements were carried out with the aid of a Nanoscope III equipped with phase extender module and vertical engage J scanner. The images were acquired in the tapping mode under ambient conditions with standard silicon cantilevers with a nominal spring constant of 50 N/m and a resonance frequency around 300 kHz. Carbon black and the grafted carbon black samples were dispersed in THF or ethanol. About 1–2 drops of the dispersions were dripped onto freshly clean silicon.

3. Results and discussion

3.1. Synthesis of CB-g-PS and CB-g-P(St-co-MA)

Usually, homopolymers and copolymers of styrene are prepared by TEMPO-mediated radical polymerization. In our experiments, polystyrene and poly(styrene-co-maleic anhydride) were synthesized using HTEMPO-mediated radical polymerization initiated by azobisisobutyronitrile or benzoyl peroxide. Polystyrene with narrow polydispersity (PDI = 1.15) was prepared by bulk polymerization of styrene initiated by AIBN in the presence of HTEMPO. Poly(styrene-co-maleic anhydride) with narrow polydispersity (PDI = 1.41) was synthesized by radical polymerization initiated by BPO in the presence of HTEMPO. Fig. 1 shows the 1H NMR spectra of HTEMPO-PS and HTEMPO-P(St-co-MA). Park et al. reported that methane peaks of MA units in the P(St-co-MA) were observed at 3.0–3.7 ppm until the MA concentration increased to 17.5 mol% [26]. Here, corresponding methane peaks of MA units could not be observed possibly because the MA concentration was relatively low.

Fig. 2 shows the FT-IR spectra of HTEMPO-PS and HTEMPO-P(St-co-MA). For HTEMPO-PS, a peak at 3431 cm^{-1} was attributed to the stretching vibration of hydroxyl group from terminal HTEMPO moiety, and the peaks at 3064 cm^{-1} , 3024 cm^{-1} , 2920 cm^{-1} , 2851 cm^{-1} , 754 cm^{-1} and 697 cm^{-1} were the characteristic peaks of polystyrene. For HTEMPO-P(St-co-MA), a strong peak at 1780 cm^{-1} was assigned to the stretching vibration of carboxyl group and a

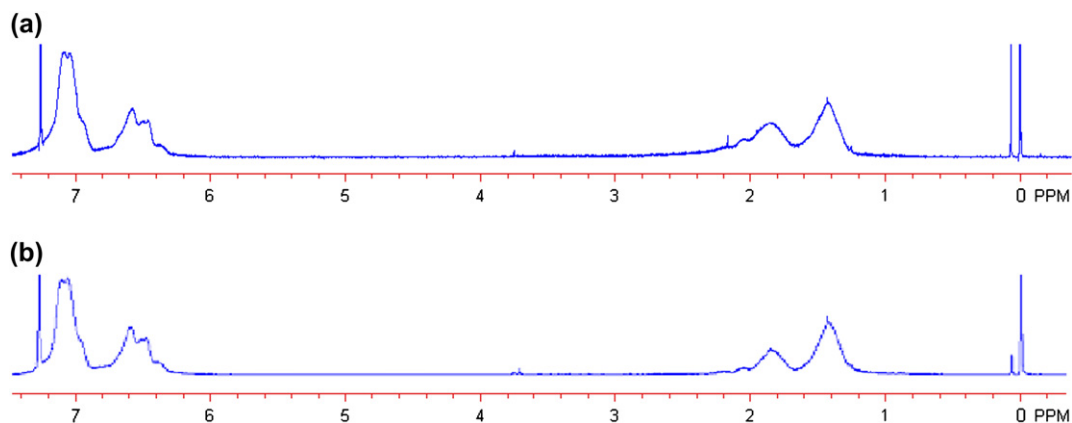


Fig. 1. 1H NMR spectra of HTEMPO-PS (a) and HTEMPO-P(St-co-MA) (b) in $CDCl_3$.

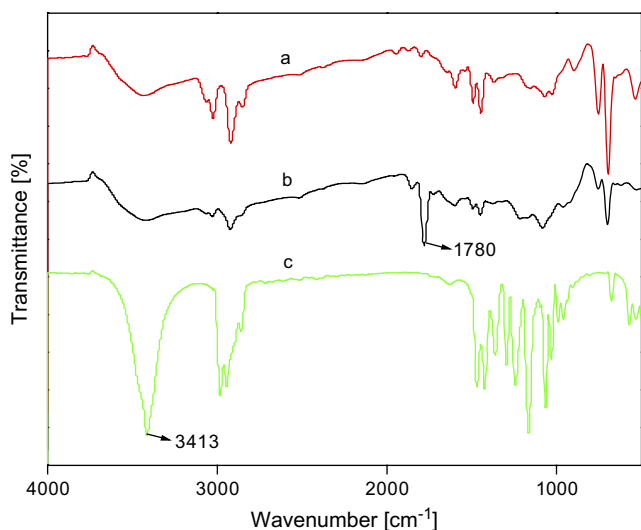
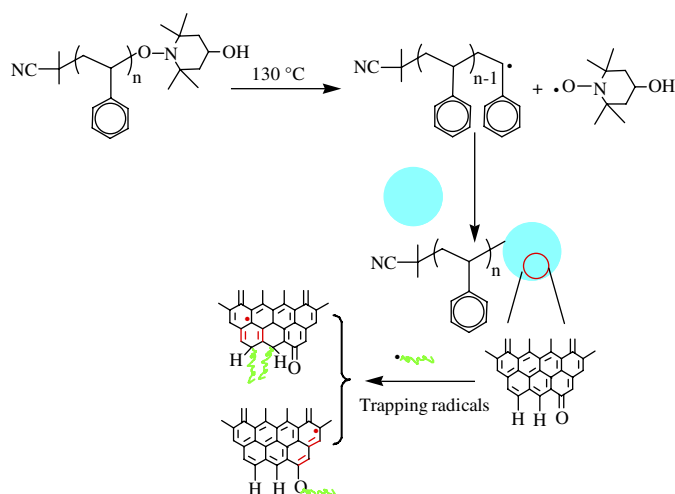


Fig. 2. FT-IR spectra of HTEMPO-PS, HTEMPO-P(St-co-MA) and HTEMPO. a: HTEMPO-PS, b: HTEMPO-P(St-co-MA), c: HTEMPO.

peak at 3422 cm^{-1} was attributed to the stretching vibration of hydroxyl group from terminal HTEMPO moiety.

When polystyrene without terminal TEMPO moiety is heated in the presence of carbon black, as a result, no polystyrene is found to be grafted onto carbon black surface because polystyrene radical is not produced during the whole process [21]. Considering that HTEMPO-terminated polymers may be dissociated thermally and polycondensed aromatic rings can trap the produced polymer radicals, HTEMPO-terminated



Scheme 1. A possible mechanism of trapping polymer radicals by carbon black surface.

polymers are used to modify carbon black. Many studies showed that carbon black was a strong radical scavenger because of its quinonic oxygen groups and unsaturated hydrogen atoms from the polycondensed aromatic rings. Radicals can attack the two kinds of double bonds from the polycondensed aromatic rings and quinonic oxygen groups, and delocalized radicals have been confirmed by ESR. Taking the trapping of polystyrene radicals as an example, a possible mechanism of trapping radicals by carbon black surface is demonstrated in Scheme 1 [21].

Since the carbon black grafted with polystyrene has good solubility in solvent, ^1H NMR spectroscopy may be used to characterize the polystyrene grafted onto carbon black surface. Fig. 3 shows the spectrum of CB-g-PS. The spectrum of CB-g-PS was nearly similar to that of pure polystyrene. The very small peaks below 1 ppm in Fig. 3 were assigned to the $-\text{CH}_3$ of the alkoxyamine initiator fragments (HTEMPO). So, trace nitroxide radical fragments may also be trapped by carbon black. The same phenomenon was similarly observed in the PS grafted onto single-walled carbon nanotubes [24].

Fig. 4a shows the thermogravimetric (TGA) curves of carbon black, polystyrene and CB-g-PS. Carbon black remained basically stable below 685 °C , however, it had about 6.49% between 685 °C and 800 °C . Pure polystyrene was mostly decomposed before 448 °C . For the weight loss curves of CB-g-PS, there were two main regions. The first region below 466 °C was the weight loss of polystyrene in CB-g-PS. Interestingly, the end decomposition temperature in some CB-g-PS samples was slightly higher than that of pure polystyrene. In the second region between 466 °C and 800 °C was carbon black remained basically stable. For CB-g-PS, as a whole, the decomposition curve was similar to that of pure polystyrene. For CB-g-PS, with the reaction continuing from 3 h to 24 h, the polystyrene content in CB-g-PS increased accordingly from 4.44% to 19.60%.

Fig. 4b shows the TGA curves of P(St-co-MA) and CB-g-P(St-co-MA). P(St-co-MA) was mostly decomposed between 367 °C and 454 °C . For CB-g-P(St-co-MA), there were also two main regions. The first region below 480 °C was the weight loss of P(St-co-MA) in CB-g-P(St-co-MA). For CB-g-P(St-co-MA), the decomposition curve was basically similar to that of pure poly(styrene-co-maleic anhydride) as a whole. However, some CB-g-P(St-co-MA) samples had relatively different weight loss curves and had higher decomposition temperature than that of pure P(St-co-MA). In the second region between 480 °C and 800 °C was carbon black remained basically stable.

The content of poly(styrene-co-maleic anhydride) in CB-g-P(St-co-MA) increased from 4.88% to 31.76% when time

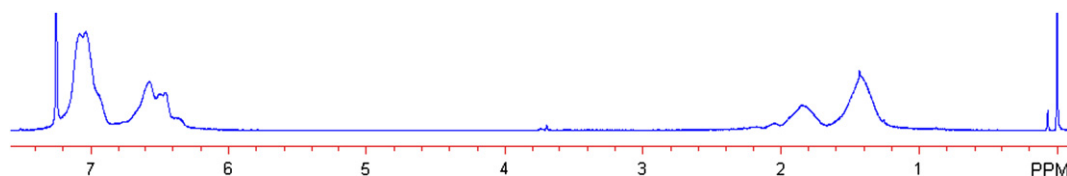


Fig. 3. ^1H NMR spectrum of CB-g-PS in CDCl_3 .

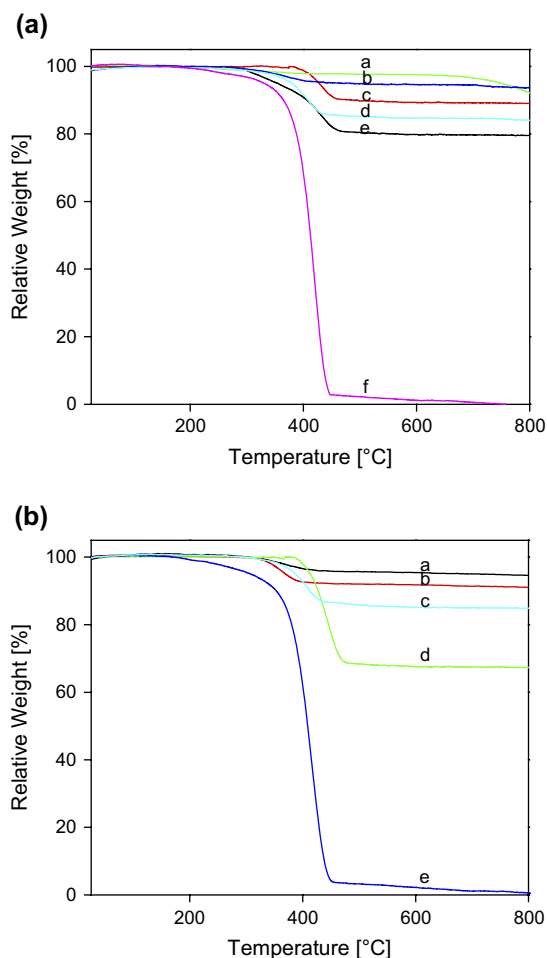


Fig. 4. (a) TGA curves of carbon black, HTEMPO-PS and CB-g-PS. a: carbon black, b: CB-g-PS-1, c: CB-g-PS-2, d: CB-g-PS-3, e: CB-g-PS-4, f: HTEMPO-PS. (b) TGA curves of HTEMPO-P(St-co-MA) and CB-g-P(St-co-MA). a: CB-g-P(St-co-MA)-1, b: CB-g-P(St-co-MA)-2, c: CB-g-P(St-co-MA)-3, d: CB-g-P(St-co-MA)-4, e: HTEMPO-P(St-co-MA).

changed from 3 h to 24 h. However, Tsubokawa et al. reported that the polystyrene content increased no further after 12 h. They considered that previously grafted polystyrene molecular chains on carbon black surface hindered the approach of subsequent polystyrene radicals [21]. In our experiment, after reaction for 12 h, the polystyrene and poly(styrene-co-maleic anhydride) contents still increased possibly owing to relatively low molecular weight.

Differential scanning calorimeter (DSC) was also utilized to characterize the carbon black grafted with polystyrene by studying the glass transition temperature (T_g) of polystyrene. Fig. 5 shows the DSC curves of CB-g-PS. It was observed that T_g became more obvious with the polystyrene content increasing in CB-g-PS.

Dynamic light scattering (DLS) was used to characterize the average sizes of carbon black, CB-g-PS and CB-g-P(St-co-MA). Pristine carbon black was strongly hydrophobic, aggregated easily in THF, and showed broad particle size distributions. However, for CB-g-PS and CB-g-P(St-co-MA), their diameters were between 126 nm and 198 nm (see in

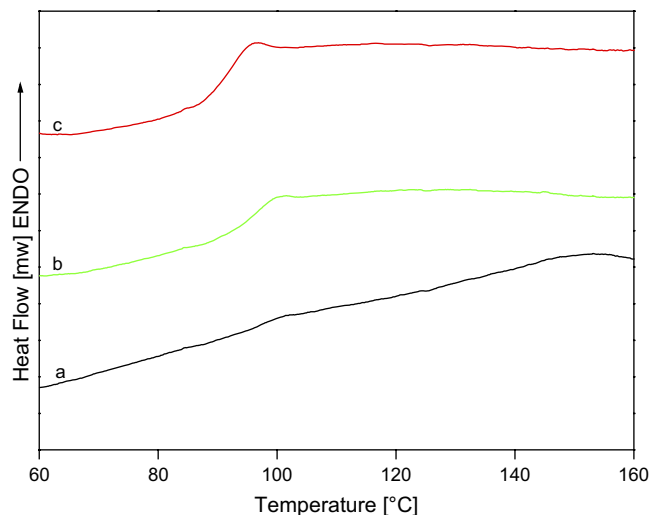


Fig. 5. DSC curves of CB-g-PS. a: CB-g-PS-1, b: CB-g-PS-2, c: CB-g-PS-3. Heating rate of 20 °C/min, cooling rate of 80 °C/min.

Table 1), and had relatively narrow size distributions. After grafted with polystyrene or poly(styrene-co-maleic anhydride), carbon black could be stable in THF because of steric stabilization supplied by polystyrene or poly(styrene-co-maleic anhydride) molecules.

Morphologies of carbon black and CB-g-P(St-co-MA) were studied by atomic force microscopy (AFM) and transmission electron microscopy (TEM). Fig. 6 shows TEM images and AFM images of carbon black and CB-g-P(St-co-MA). Carbon black was not dispersible in THF and existed with large agglomerates. CB-g-P(St-co-MA) tended to form film or cross-linked structures possibly due to the hydrolysis of MA in THF [29].

Carbon black is strongly hydrophobic and cannot be well dispersed in THF. However, CB-g-PS and CB-g-P(St-co-MA) have good solubility in THF. Fig. 7 shows the solubility photo of CB-g-PS and CB-g-P(St-co-MA) in THF. After standing for two months, CB-g-PS and CB-g-P(St-co-MA) could exist stably in THF.

3.2. Synthesis of CB-g-P(St-co-4VP) and CB-g-P4VP

Apart from styrene and its derivatives, nitroxide-mediated radical polymerization is also applicable for vinylpyridine. Fischer et al. reported the synthesis of 4-vinylpyridine by TEMPO [28]. The nucleophilic basic nitrogen atom of 4-vinylpyridine can be quaternized by iodomethane and quaternization of polymer chain leads to high solubility in neutral water, which is beneficial to synthesize amphiphilic and water-dispersed carbon black [30]. Here, poly(4-vinylpyridine) and the random copolymer of styrene and 4-vinylpyridine were synthesized using the HTEMPO-mediated radical polymerization initiated by BPO or AIBN. Fig. 8 shows the ^1H NMR spectra of P(St-co-4VP) and P4VP. The relatively small peaks at 0.95 ppm were assigned to the $-\text{CH}_3$ of the alkoxyamine initiator fragments at the ends of poly[styrene-co-(4-vinylpyridine)] or poly(4-vinylpyridine) chains.

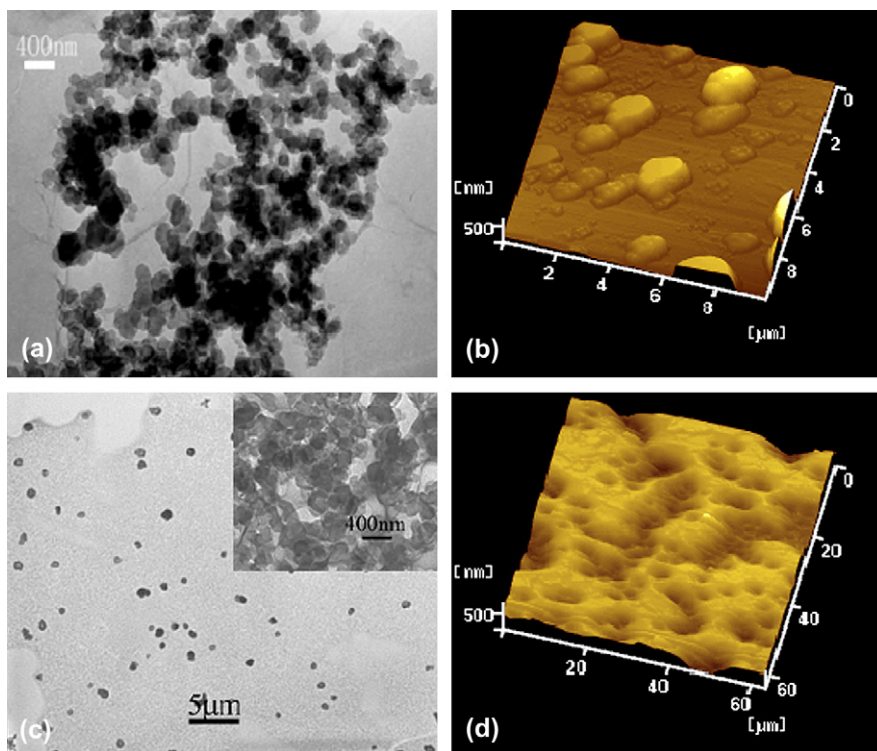


Fig. 6. TEM images and AFM images of carbon black and CB-g-P(St-co-MA). (a,b): carbon black, (c,d): CB-g-P(St-co-MA).

Fig. 9 shows the FT-IR spectra of HTEMPO-P4VP and HTEMPO-P(St-co-4VP). For HTEMPO-P4VP, three peaks at 1596 cm^{-1} , 1412 cm^{-1} and 993 cm^{-1} were assigned to the characteristic peaks of P4VP, and a peak at 3409 cm^{-1} was attributed to the stretching vibration of hydroxyl group from terminal HTEMPO moiety of P4VP. For HTEMPO-P(St-co-4VP), a

peak at 3412 cm^{-1} was attributed to the stretching vibration of hydroxyl group from terminal HTEMPO moiety of P(St-co-4VP) and the peak at 993 cm^{-1} was assigned to pyridine ring absorption.

Fig. 10a shows the TGA curves of carbon black, P(St-co-4VP) and CB-g-P(St-co-4VP). P(St-co-4VP) was mainly decomposed before $469\text{ }^{\circ}\text{C}$. The decomposition curve of P(St-co-4VP) in CB-g-P(St-co-4VP) was similar to that of pure P(St-co-4VP). P(St-co-4VP) in CB-g-P(St-co-4VP) was decomposed completely before $593\text{ }^{\circ}\text{C}$. However, all CB-g-P(St-co-4VP) samples had slightly different weight loss curves. The P(St-co-4VP) content in CB-g-P(St-co-4VP) was between 10.60% and 24.13%.

Fig. 10b shows the TGA curves of carbon black, P4VP and CB-g-P4VP. Pure P4VP was mostly decomposed before $432\text{ }^{\circ}\text{C}$. For CB-g-P4VP, there were two main regions in the weight loss curve. The first region below $458\text{ }^{\circ}\text{C}$ was the weight loss of P4VP in CB-g-P4VP. In the second region between $458\text{ }^{\circ}\text{C}$ and $800\text{ }^{\circ}\text{C}$ carbon black remained stable. The P4VP content in CB-g-P4VP was between 14.08% and 20.32% (Table 2).

Fig. 11 shows the AFM images of CB-g-P4VP and CB-g-P(St-co-4VP). Their morphologies were different from carbon black. CB-g-P4VP and CB-g-P(St-co-4VP) could be well dispersed in ethanol and existed with nanometer-sized agglomerates. The diameter of single agglomerate of CB-g-P4VP was also calculated by AFM. In Fig. 10a, the three CB-g-P4VP agglomerates' diameters were, respectively, 211 nm, 305 nm and 317 nm, which were consistent with the results obtained by dynamic light scattering.

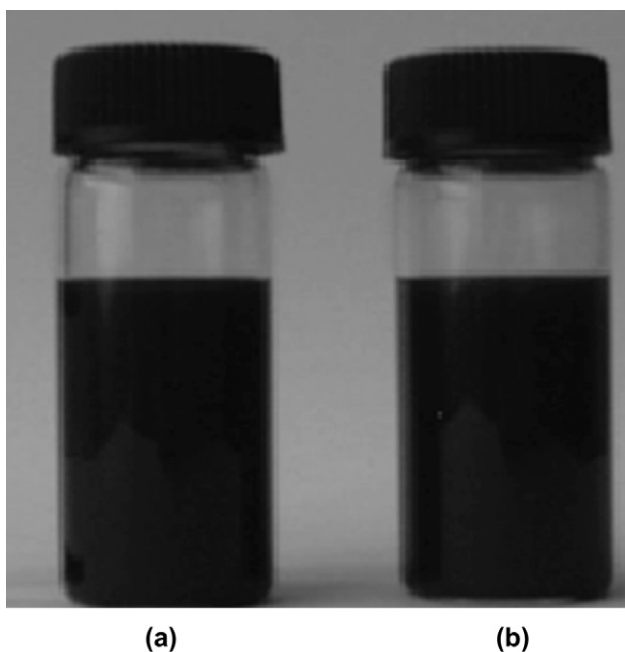


Fig. 7. Solubility photo of CB-g-PS and CB-g-P(St-co-MA). a: CB-g-PS, b: CB-g-P(St-co-MA).

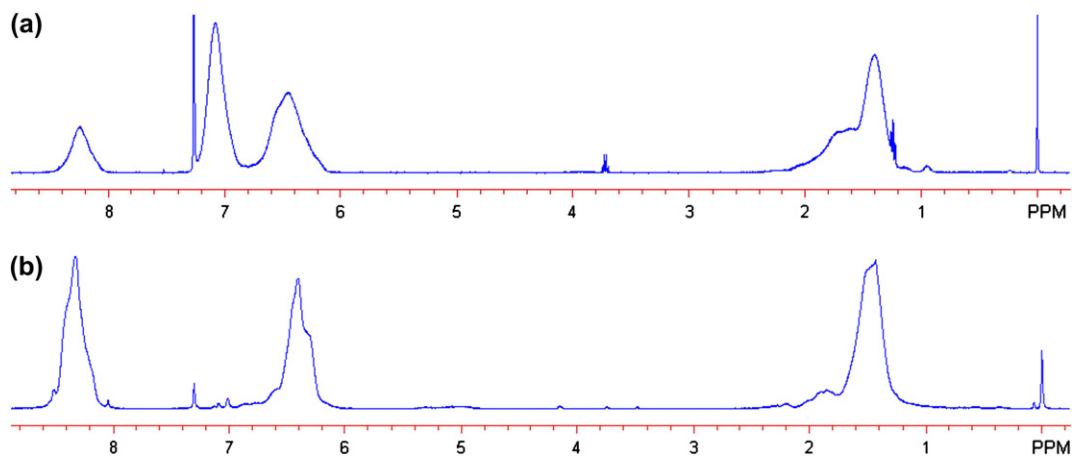


Fig. 8. ^1H NMR spectra of HTEMPO-P(St-co-4VP) (a) and HTEMPO-P4VP (b) in CDCl_3 .

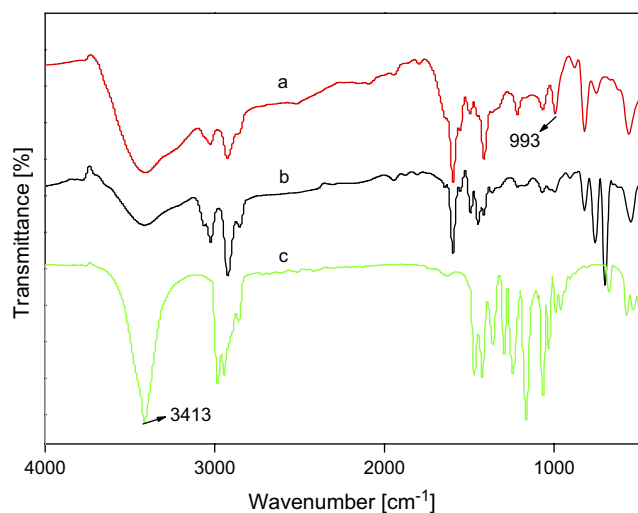


Fig. 9. FT-IR spectra of HTEMPO-P4VP, HTEMPO-P(St-co-4VP) and HTEMPO. a: HTEMPO-P4VP, b: HTEMPO-P(St-co-4VP), c: HTEMPO.

Table 2

Reaction conditions and results

Sample	Time (h)	R	Polymer (%)	Particle size (nm)
CB-g-P(St-co-4VP)-1	6	4	10.60	287
CB-g-P(St-co-4VP)-2	12	4	14.04	203
CB-g-P(St-co-4VP)-3	12	10	20.63	267
CB-g-P(St-co-4VP)-4	12	15	24.13	272
CB-g-P4VP-1	12	4	14.08	200
CB-g-P4VP-2	12	10	15.81	310
CB-g-P4VP-3	12	15	20.32	317

Reaction conditions: temperature = $130\text{ }^\circ\text{C}$; CB = 50 mg; DMF = 2 ml. PS:P4VP = 7:6, calculated by ^1H NMR. R = the weight ratio of HTEMPO-polymer/CB (w/w). HTEMPO-P(St-co-4VP): $M_n = 8.1 \times 10^3$, PDI = 1.27, determined by GPC; HTEMPO-P4VP: $M_n = 8.3 \times 10^3$, PDI = 1.20, determined by GPC. Polymer (%) = the polymer content, calculated from TGA under N_2 . Particle size was measured from dynamic light scattering in ethanol.

Fig. 12 shows the solubility photo of CB-g-P(St-co-4VP) and CB-g-P4VP in ethanol. Carbon black cannot be dispersed in ethanol. However, CB-g-P(St-co-4VP) and CB-g-P4VP have good solubility in ethanol.

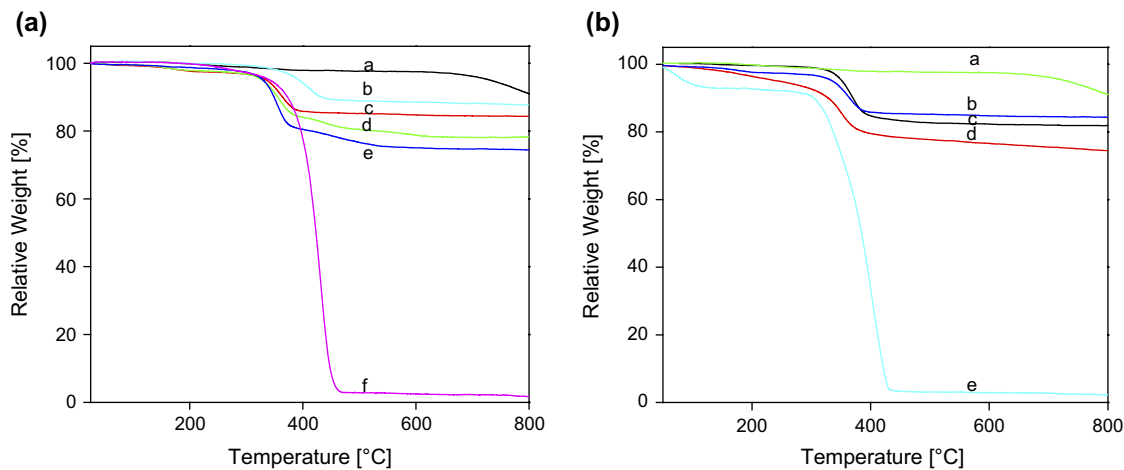


Fig. 10. (a) TGA curves of CB-g-P(St-co-4VP). a: carbon black, b: CB-g-P(St-co-4VP)-1, c: CB-g-P(St-co-4VP)-2, d: CB-g-P(St-co-4VP)-3, e: CB-g-P(St-co-4VP)-4, f: HTEMPO-P(St-co-4VP). (b) TGA curves of CB-g-P4VP. a: carbon black, b: CB-g-P4VP-1, c: CB-g-P4VP-2, d: CB-g-P4VP-3, e: HTEMPO-P4VP.

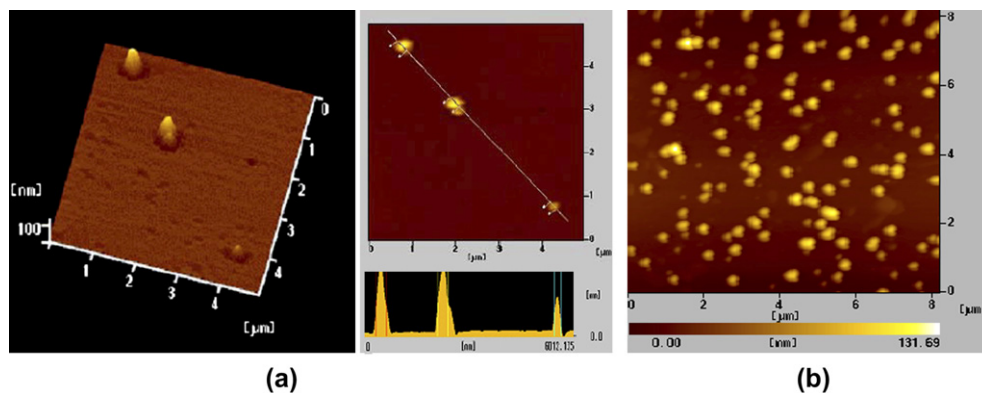


Fig. 11. AFM images of CB-g-P(St-co-4VP) and CB-g-P4VP. (a): CB-g-P4VP, (b): CB-g-P(St-co-4VP).



Fig. 12. Solubility photo of CB-g-P(St-co-4VP) and CB-g-P4VP in ethanol after standing for two months, a: CB-g-P(St-co-4VP), b: CB-g-P4VP.

4. Conclusion

Four kinds of well-defined polymers were synthesized using HTEMPO-mediated radical polymerization initiated by AIBN or BPO. These polymers were grafted onto carbon black surface by the radical trapping method. The grafted carbon black was systematically characterized. Dispersion experiments showed that the carbon black grafted with polymers could be well dispersed in various organic solvents. Especially, the carbon black grafted with poly(4-vinylpyridine) can become hydrophilic if further quarternized with iodomethane. These grafted carbon black nanoparticles may be useful candidates for developing sensor materials and their gas sensing characteristics are under investigation.

References

- [1] Lonergan MC, Severin EJ, Doleman BJ, Beaver SA, Grubbs RH, Lewis NS. *Chem Mater* 1996;8:2298.
- [2] You T, Niwa O, Tomita M, Hirono S. *Anal Chem* 2003;75:2080.
- [3] Sotzing GA, Briglin SM, Grubbs RH, Lewis NS. *Anal Chem* 2000;72:3181.
- [4] Dickert FL, Haunschild A. *Adv Mater* 1993;5:887.
- [5] Lewis NS. *Acc Chem Res* 2004;37:663.
- [6] Chen SG, Hu JW, Zhang MQ, Li MW, Rong MZ. *Carbon* 2004;42:645.
- [7] Wu GZ, Asai S, Sumita M. *Macromolecules* 2002;35:945.
- [8] Tsubokawa N. *J Macromol Sci Chem* 1987;24:763.
- [9] Tsubokawa N. *J Polym Sci Polym Chem Ed* 1984;22:1515.
- [10] Tsubokawa N. *J Polym Sci Part A Polym Chem* 1987;25:1979.
- [11] Tsubokawa N, Yu J, Yasuo S. *J Polym Sci Part A Polym Chem* 1988;26:2715.
- [12] Tsubokawa N, Funaki A, Sone Y. *J Appl Polym Sci* 1983;8:2381.
- [13] Hayashi S, Handa S, Tsubokawa N. *J Polym Sci Part A Polym Chem* 1996;34:1589.
- [14] Tsubokawa N, Fujiki K, Sone Y. *Polym J* 1988;20:213.
- [15] Li W, Xie Z, Li Z. *J Appl Polym Sci* 2001;81:1100.
- [16] Jin YZ, Gao C, Kroto HW, Maekawa T. *Macromol Rapid Commun* 2005;26:1133.
- [17] Li L, Lukehart CM. *Chem Mater* 2006;18:94.
- [18] Liu TQ, Jia SJ, Matyjaszewski K. *Langmuir* 2003;19:6342.
- [19] Liu TQ, Casado-portilla R, Belmont J, Matyjaszewski K. *J Polym Sci Part A Polym Chem* 2005;43:4695.
- [20] Liu TQ, Jia SJ, Kowalewski T, Matyjaszewski K, Casado-portilla R, Belmont J. *Macromolecules* 2006;39:548.
- [21] Yoshikawa S, Machida S, Tsubokawa N. *J Polym Sci Part A Polym Chem* 1998;36:3165.
- [22] Lee CF, Yang CC, Wang LY, Chiu WY. *Polymer* 2005;46:5514.
- [23] Hayashi SJ, Naitoh A, Machida S, Okazaki M, Maruyama K, Tsubokawa N. *Appl Organomet Chem* 1998;12:743.
- [24] Liu YQ, Yao ZL, Adronov A. *Macromolecules* 2005;38:1172.
- [25] Greszta D, Matyjaszewski K. *Macromolecules* 1996;29:7661.
- [26] Park ES, Kim MN, Lee IM, Lee HS, Yoon JS. *J Polym Sci Part A Polym Chem* 2000;38:2239.
- [27] Chen ZJ, Wang Y, Feng Y, Jiang XQ, Yang CZ, Wang M. *J Appl Polym Sci* 2004;91:1842.
- [28] Fisher A, Brembilla A, Lochon P. *Macromolecules* 1999;32:6069.
- [29] Zhou JF, Wang L, Wang CL, Chen T, Yu HJ, Yang Q. *Polymer* 2005;46:11157.
- [30] Matsuno R, Yamamoto K, Otsuka H, Takahara A. *Macromolecules* 2004;37:2203.